Use of rock mechanics laboratory data in geomechanical modelling to increase confidence in CO$_2$ geological storage

Peter Olden[*], Gillian Pickup, Min Jin, Eric Mackay, Sally Hamilton, James Somerville, Adrian Todd

Heriot-Watt University, Institute of Petroleum Engineering, Edinburgh EH14 4AS, Scotland, UK

A B S T R A C T

One of the many challenges facing carbon capture and storage will be to provide convincing evidence of the geomechanical integrity of any proposed geological storage site. Contrary to storage in depleted hydrocarbon fields, storage in saline aquifer presents many more unknowns in this respect because there will probably be no known previous pressure response history or rock property characterisation. The work presented here was carried out as part of a project investigating the improvement in levels of confidence in all aspects of site selection and characterisation that could be expected with increasing data availability for saline aquifers. Attention here was focused on geomechanical modelling and the rock mechanics data used to populate these models. The models initially used generic geomechanical property data and the potential for shear failure of the intact rock and (fault) reactivation of fractured rock investigated. The models were then updated with laboratory measured rock mechanical properties for actual rock from the proposed storage system locality. The modelled results were changed marginally but did not identify any significant issues of criticality because of the relative geomechanical "benignness" of the storage site.

1. Introduction

Carbon capture and storage (CCS) faces many challenges – among them the validation of safety and quantification of risks associated with any geological storage element. To quantify those risks a thorough understanding of the subsurface chemico-physical processes involved is required together with a capability to simulate them for storage evaluation and design purposes. Although much information can be gathered from other geo-engineered and natural subsurface production/storage activity, the validation of CO$_2$ geological storage brings together requirements at the forefront of many disciplines. This is particularly so in the area of reservoir simulation, where the once considered sufficient hydrogeological flow modelling for hydrocarbon reservoirs, must be augmented by the modelling of both geochemical and geomechanical processes. In many CO$_2$ geological storage projects the current methodology is to investigate these processes independently. However they are intrinsically linked and the goal in reservoir simulation for CO$_2$ geological storage must be to develop modelling methods and techniques that capture the interdependence of all processes involved including flow, thermal, geochemical and geomechanical effects.

Geomechanical effects are recognised as being significant in the behaviour of many producing hydrocarbon reservoirs as dramatically illustrated by the compaction and subsidence in fields such as the Wilmington oilfield in California and Ekofisk in the North Sea. An extensive literature documenting reservoir geomechanics has developed and geomechanical modelling is now recognised as integral part of characterising and simulating the behaviour of many producing hydrocarbon reservoirs. As effort continues to extend the scope of reservoir simulation for CO$_2$ geological storage it will also be necessary to incorporate geomechanical modelling capabilities for the particular requirements of this type of geo-engineering.

When CO$_2$ is injected into a porous and permeable formation, it will be forced into the rock pores at a higher pressure than is present in the surrounding rock. This causes changes to the stress state of the rock mass leading to deformation and possible failure of the reservoir and/or seal rock. Pre-existing fractures or faults may be opened up and/or new fractures or faults created, potentially providing conduits for leakage. The conditions under which this may happen are site specific and depend on the injection pressures utilised, the characteristics of the host formation, the in situ stress regime and the production history of the reservoir.

The most immediate risk to leakage in CO$_2$ geological storage is posed by breaching the caprock. However reactivation may also take place on faults within and transecting the reservoir. An important observation as regards modelling is that the geomechanical domain or region of influence will be much greater than that influenced by just the CO$_2$ plume itself or indeed any induced pressure

* Corresponding author. Tel.: +44 0 131 451 3172; fax: +44 0 131 451 3127.
  E-mail address: peter.olden@pet.hw.ac.uk (P. Olden).

changes, so a geomechanical model based on just the flow domain alone may not capture all deleterious effects. Some geomechanical effects may not necessarily pose risks to storage integrity if they occur remotely from the contained CO_2 or migration pathways.

Although reservoir simulation is a well established tool in the exploitation of hydrocarbon reservoirs, geomechanical modelling is less practised. In the past, reservoir geomechanics was not considered a priority, with many reservoirs considered technically straight-forward and having undergone only limited depletion and/or pressure support. However, declining resource volumes and increasing oil prices have prompted operators to seek less accessible prospects in formations with higher pressures, higher temperatures and in potentially tectonically active regions. The modelling tools developed in these situations can usefully be applied to CO_2 geological storage.

CO_2 storage in depleted hydrocarbon fields – through enhanced oil and gas recovery projects – has provided the precursor to the CO_2 geological storage industry, but storage in saline aquifers will likely be the main focus of attention in the future due to the significantly greater potential storage capacities they provide. The most extensive theoretical study to date, modelling geomechanical effects in relation to saline aquifer storage has been carried out by Rutqvist and others (Rutqvist et al., 2007, 2008; Rutqvist and Tsang, 2002). The potential for fracture initiation and reactivation of existing fractures was analysed in different in situ stress regimes, commencing with isotropic and normal faulting (extensional) and then extending to a reverse faulting (compressional) regime in a multilayered system. The type of initial stress is a key parameter that determines whether fracturing or shear slip take place sub-horizontally or sub-vertically and in which location. Rutqvist also provides a comprehensive review of the major factors related to geomechanics in the CO_2 storage in deep sedimentary formations (Rutqvist, 2012).

A large body of work in (hydrocarbon) reservoir geomechanics is described in terms of "geomechanical modelling", "mechanical earth modelling" or other similar terms. A mechanical earth model has been defined as a logical compilation of relevant information about earth stresses and rock mechanical properties based on geomechanical studies and geological, geophysical and reservoir engineering models (Jimenez et al., 2005). It is important to understand that a model in these terms may not specifically refer to modelling in the sense of the simulation of reservoir geomechanical behaviour using numerical modelling software. The geomechanical model may be more accurately described as a geomechanical characterisation, although a degree of analytical modelling may be incorporated in the process. It is in this latter category that a significant amount of work has been done in relation to the geomechanical modelling of subsurface CO_2 storage. A good example of the development of a geomechanical model (or characterisation) of a storage site using the methods described above is given in (Lucier et al., 2006). The paper describes in detail the determination of the in situ stress state from well logs using the methodology given by (Zoback et al., 2003).

Australia's GEODISC research program into the safe storage of CO_2 in saline aquifers and depleted hydrocarbon reservoirs has also concerned itself with geomechanical modelling (Streit and Hillis, 2003, 2004; Streit and Siggins, 2005; Streit et al., 2005) and focused on the maximum sustainable formation pressures that will not reactivate existing faults or induce new fractures. The methodology used is also based on the Mohr–Coulomb failure criterion and was originally developed as an algorithm for estimating fluid pressures that can induce fault reactivation during depletion in hydrocarbon reservoirs (Streit and Hillis, 2002, 2003).

Recent activity in the area of geomechanical modelling of CO_2 storage in saline aquifers has focussed on the In Salah project in Algeria (Ringrose et al., 2009). The project is distinctive in that

ground surface (uplift) deformations measured by satellite airborne radar interferometry (InSAR) can be directly linked to the injection of CO_2 through three horizontal wells. The project is providing a test bed for different modelling approaches from various investigators with efforts being made to match both the magnitude and pattern of surface displacements(Bissell et al., 2011; Morris et al., 2009, 2011; Preisig and Prévost, 2011; Rutqvist et al., 2009, 2010). Recent concerns have been raised over the potential triggering of human detectable seismic events (Cappa and Rutqvist, 2011), as has been observed in some hydraulic fracturing and other gas storage projects.

One of the main challenges of geomechanical modelling is the gathering and assessment of rock mechanical data. A limited appraisal of a particular site can be made using generic data but to increase confidence in safety and security, site specific data are required. The work described here investigates this process.

2. Geomechanical models

There are various approaches to reservoir simulation incorporating geomechanical effects. A coupled analysis whereby there is feedback from the geomechanical model to the flow model is now considered the preferred method. The stress and strain state of the geomechanical model is used to modify the hydraulic properties (porosity and permeability) of the flow model according to (usually) empirical relationships. The exchange of data between the two simulations can be scheduled to take place at different times according to the magnitude of say, the pore pressure changes taking place. A fully coupled analysis all conducted within the same code in which the flow and deformation calculations are solved simultaneously is the most rigorous type of simulation but there may be a heavy computational requirement. The former method was used here.

The geomechanical models were developed from reservoir simulation models of sub-surface CO_2 injection into a saline aquifer at a hypothetical storage site based on the geology to be found just onshore the North Sea coast of Lincolnshire, England. The target storage aquifer formation was the Sherwood Sandstone Group (average porosity 20% and permeability 500 mD) with thicknesses up to 300 m, overlain by the Mercia Mudstone Group as caprock, and underlain by the Roxby sealing formation. Injection of super-critical CO_2 was projected to take place at a depth of around 1200 m i.e. below the 800 m threshold that any phase change to free gas might occur. The CO_2 plume was anticipated to migrate up-dip to the SSW through gently dipping beds, with the primary trapping mechanism expected to be residual, with some structural trapping at sealing sub-vertical faults. The reservoir models themselves were developed as part of a multi-disciplinary project CASSEM (CO_2 Aquifer Storage Site Evaluation and Monitoring) covering all aspects of the CCS chain (Smith et al., 2011).

The reservoir modelling methodology and models were progressed in various stages according to data availability and modelling complexity (Pickup et al., 2011). The geomechanical models are described here as "preliminary models", referring to the use of published geomechanical property data together with the intermediate stage reservoir models of the CASSEM project, and "updated models" referring to the use of site specific laboratory derived geomechanical property data, together with the final stage reservoir models of the project. The VISAGE coupled reservoir geomechanical simulation software was used for the geomechanical modelling (Schlumberger, 2009).

The reservoir models of the aquifer/caprock CO_2 geological storage system were developed from a Petrel geological geo-cellular model using the ECLIPSE 300 compositional reservoir simulator. The geo-cellular model covered a study area approximately 50 km × 18 km and incorporated surfaces (significant strata
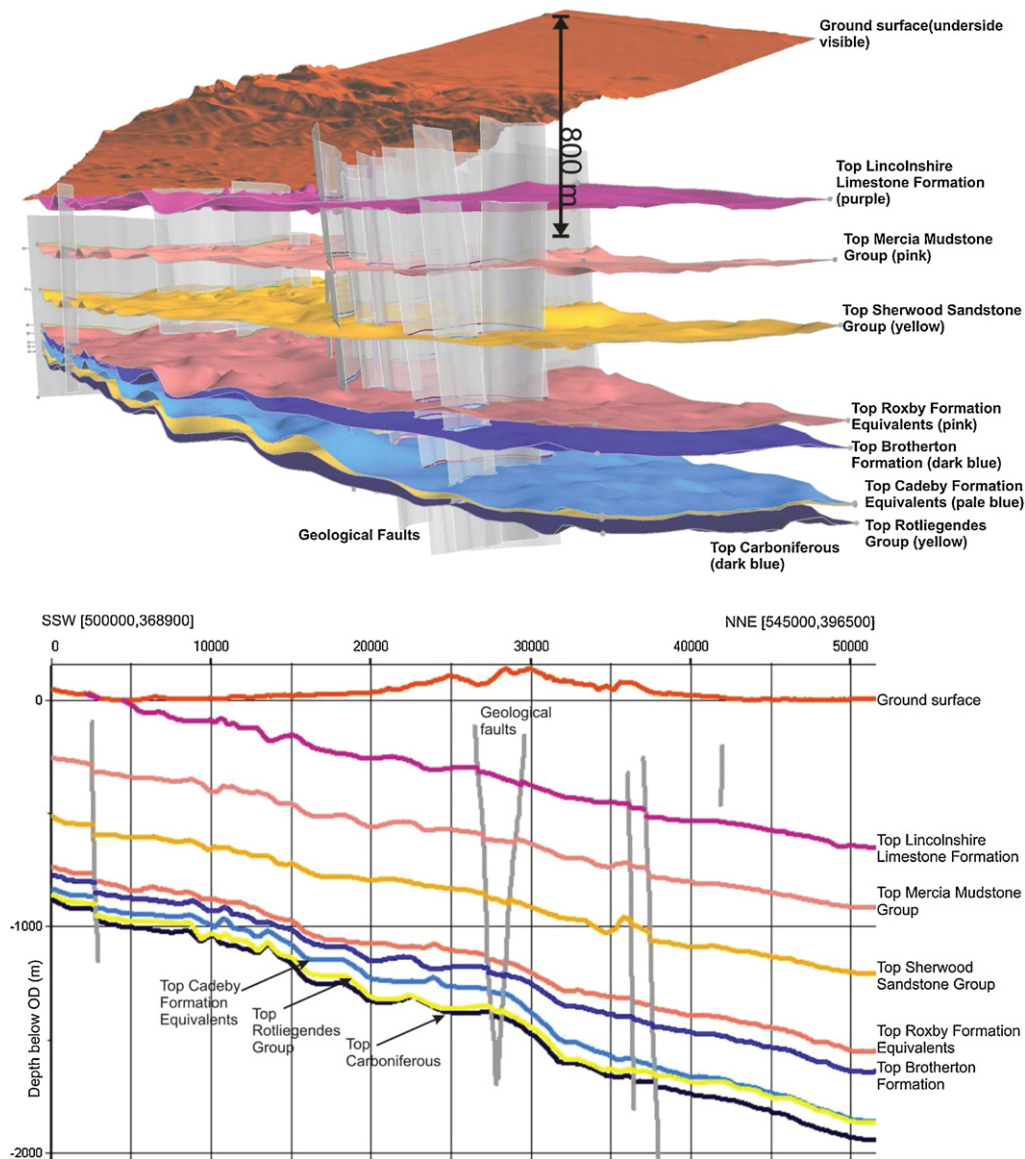
Fig. 1. Geological model of the storage site showing significant horizons and faults – (a) 3D view of the bedrock geology model viewed from the SW, looking NW and (b) cross-section running SSW–ENE through the bedrock geology model – reproduced with the permission of the British Geological Survey ©NERC. All rights reserved.

horizons) and faults. The actual geology was interpreted from a combination of 2D and 3D seismic data and was relatively straightforward with gently dipping beds of 1–2° inclination to the horizontal. The presence of a group of sub-vertical faults with negligible throws was interpreted in the central region of the model. The geological model is shown in Fig. 1.

The reservoir model was populated with representative stochastic distributions of porosity and permeability based on well log data from within the study area. Distributions were required for three zones – a caprock consisting predominantly of mudstone (Mercia Mudstone Group), the target storage aquifer consisting of sandstone (Sherwood Sandstone group) and a basal formation (Roxby formation) as shown in Fig. 2. The faults in the central region of the model were treated as transmissibility barriers.

The ECLIPSE 300 models were run using the CO2STORE option which treats the displacement and solubility interaction of the CO_2 with the brine consisting of the dissolved salts sodium chloride, calcium chloride or calcium carbonate. Nearby borehole data was used for brine composition. Usually when simulating CO_2 storage, only a small part of the whole aquifer is simulated in detail, since this will be adequate to represent the final extent of the CO_2 plume

migration. However for the purpose of predicting the system pressure response it is important that the total volume of the aquifer is taken in to account. "Numerical aquifers" – large pore volumes of additional water – were connected to the grid to simulate an extended storage system. These numerical aquifers act as additional pore space to accommodate the brine displaced as a result of injecting CO_2 in to the system. Simulations were performed both with and without an extended or regional aquifer.

A single vertical well, near the east side (down-dip) of the model, was utilised for injection at a rate of 15 Mt/year over a 15 year period after which the well was shut in. In reality, 15 Mt/year could not be injected through a single well and a rate of the order 1–2 Mt/year would be more reasonable. The simulations here therefore represent CO_2 injection through a cluster of wells.

The simulation was run initially up to ~9000 years to check the extent of CO_2 migration. Typical results for CO_2 migration are also presented in Fig. 2 which shows the CO_2 gas saturation in the top layer of the aquifer. These results confirm that the free gas is concentrated at the well, spreading away at the end of the injection phase but then continues to migrate very slowly up dip with residual trapping taking place. Stratigraphic trapping also occurs at the
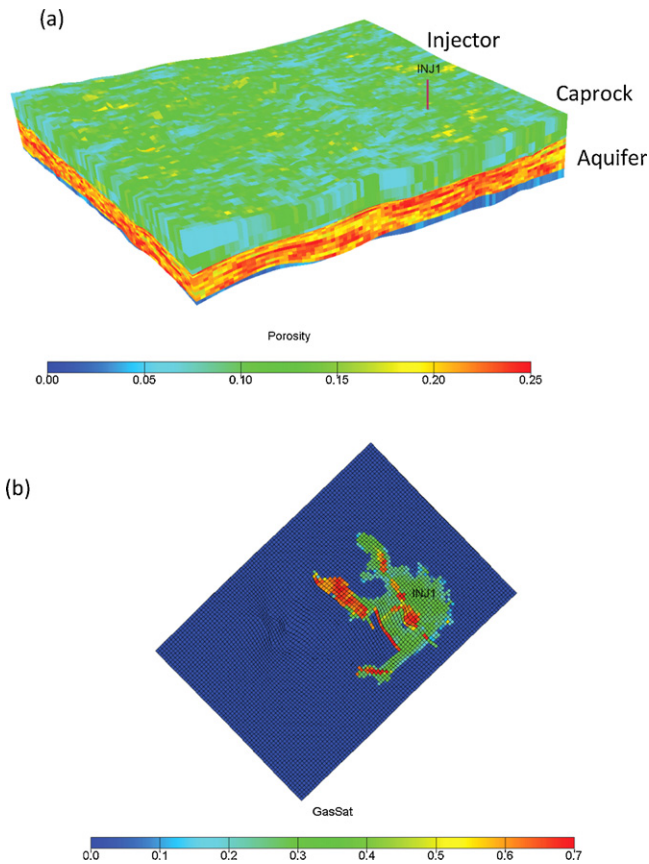
Fig. 2. Reservoir model and typical flow simulation results: (a) porosity distribution and (b) free gas saturation at top of aquifer at the end of 7000 years.

Vertical exaggeration ⊔10

Fig. 3. Example (coarse grid) of embedded geomechanical model mesh.

faults in the middle of the model which transect the general migration direction. After ~7000 years the trapped gas is still contained within the areal extent of the model.

Two models of the storage site were developed. The first model undertaken was a fine grid model of the site with areal cell size 400 m × 400 m (96,480 cells). This model however, proved to be slightly onerous on computing resources and it was decided to also work with a coarser grid model with areal cell size of 1000 m × 1000 m (21,285 cells). The input data files for the reservoir models were imported into Modeler – the VISAGE pre-processing program.

The basic function of the Modeler is to prepare the model for a coupled analysis. This involves various steps, the first of which is to "embed" the model i.e. surround it on all sides, underneath and top with extra cells which will constitute the side-, under- and overburdens respectively. Although embedding extends the model to similar dimensions as the Petrel model, outside the active reservoir model region, the precise correspondence to the geological model is lost. The main function of the embedding is to adequately capture representative geomechanical boundary conditions without introducing any extraneous effects e.g. due to irregularities in the edges of the reservoir model grid.

The cells of the embedded model are more correctly the elements of the VISAGE finite element model – in this case higher order mid-side node elements were used. Although embedding is a relatively straightforward process it needs to be done carefully to ensure an adequate but not excessive number of cells are added, that there is a smooth gradation in cell size to the model boundaries and that cells sizes are not excessively large or small. Elements of very high aspect ratio need to be avoided where significant stress changes are anticipated. Provided very high aspect ratio
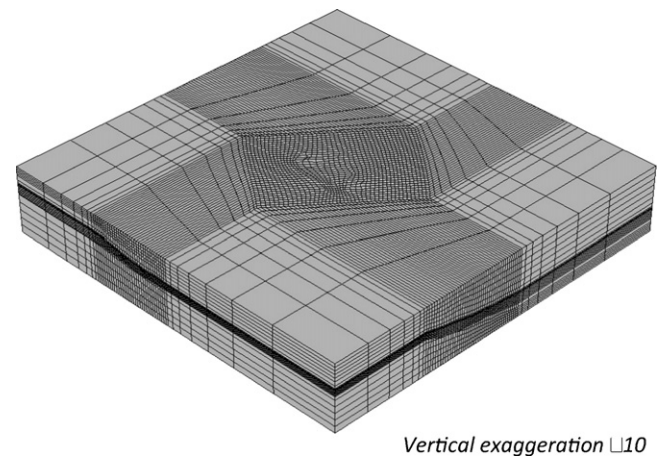
elements are kept to the periphery of the geomechanical model the analysis should still be satisfactory. The embedded fine grid model was 232,400 cells and the coarse grid model 66,975 cells. Overall the geomechanical models extended from the surface at 0 m to 2000 m depth, with this embedding depth considered adequate to not introduce any edge effects. An example embedded model grid is shown in Fig. 3.

2.1. Mechanical properties

The second stage in the development of the geomechanical models was to assign appropriate geomechanical properties to the various regions of the model. The geomechanical properties were derived from published data, developing correlations for both elastic deformation parameters – Young's modulus E and Poisson's ratio ν – and (Mohr–Coulomb) failure parameters – cohesion S_o and angle of internal friction ϕ – against porosity[1]. Two groups of correlations were developed, one for the aquifer layers in the models assumed to be sandstone and another for the caprock layers, assumed to be mudstone. For the aquifer layers of the models the correlations were based on extensive sandstone data (Edlmann, 2001) and for the caprock on the more limited North Sea shale data (Horsrud et al., 1998) (Horsrud, 2001) and are given in Table 1.

Table 1
Published geomechanical property correlation data for sandstone and shales.

Correlation	Source
Sandstone	
$E = 48.09 - 1.0185\,\phi$	Edlmann (2001)
$\nu = 0.0923 + 0.0032\,\phi$	Edlmann (2001)
$C_o = 132.32 - 3.2624\,\phi$	Edlmann (2001)
$k = 3.7537 - 0.0586\,\phi$	Edlmann (2001)
Shales	
$C_o = 243.6\,\phi^{-0.96}$	Horsrud (2001)
$E = 0.158\,C_o$	Horsrud et al. (1998)
$\beta = 49.8 + 0.3\,C_o$	Horsrud (2001)
$\nu = 0.1231 + 0.0041\,\phi$	Inferred from Horsrud (2001)
where	
E	Young's modulus (GPa)
ν	Poisson's ratio
C_o	Uniaxial compressive strength (MPa)
k	Triaxial stress factor
β	Failure angle (°)
ϕ	Porosity (%)

---

[1] Note the symbol "ϕ" is also used for porosity in Table 1.

Triaxial stress factor k, used in the sandstone data, is the linear slope of stress at shear failure plotted versus confining stress, for a rock samples tested in triaxial compression in the laboratory. Uniaxial compressive strength C_o will just be the failure stress at zero confining stress. The Mohr–Coulomb failure parameters S_o and ϕ required for model input data, can then be derived from C_o and k using the following transformations:

$$S_o = \frac{C_{o\,in\,situ}}{2\sqrt{k}}$$
$$\tan\phi = \frac{k-1}{2\sqrt{k}}$$
where $C_{o\,in\,situ} = \dfrac{C_o}{f}$

The in situ strength factor f, is a simple factor applied to C_o (measured in the laboratory) to convert to in situ conditions for modelling purposes. It is used because laboratory sampling of rocks will typically over-estimate strength values in real geotechnical situations.

The shale data is not quite so straightforward, as the correlations are not all against porosity. The failure parameters are given in terms of uniaxial compressive strength C_o and failure angle β. These require the following transformations to be applied:

$$S_o = \frac{C_{o\,in\,situ}}{2\tan\beta}$$
$$\phi = 2\beta - 90°$$

A value of 5 for in situ strength factor f as suggested by (Wilson, 1982) for unknown conditions, was used for both the caprock and aquifer.

The correlations for the elastic deformation and failure mechanical properties used in the models are illustrated in Fig. 4.

2.2. Stress initialisation

The geomechanical analysis calculates effective stresses, where the effective stress is the total stress minus the pore pressure. In a coupled analysis the pore pressure changes calculated by the reservoir simulation are used to modify the stresses starting from an initial effective stress state that must be set up in the geomechanical model. The simplest method of stress initialisation was used for the models whereby the initial stress state is specified or "wished" into place, rather than being induced by external loadings.

Taking the Modeler defaults, the vertical effective stresses were set using a total stress gradient of 22.6 kPa/m (1 psi/ft) and a pore pressure gradient of 10 kPa/m (0.44 psi/ft). Using this method, for the purposes of the coupled analysis, the absolute value of these gradients is not strictly important. It is the difference in these gradients which determines the initial effective stress gradient, which in this case will be 12.6 kPa/m (0.56 psi/ft).

The orientation and magnitude of the maximum and minimum horizontal stress components can be further specified. For these components the total stresses are specified in terms of multipliers of the vertical stress. In the absence of actual site borehole data, the World Stress Map (Heidbach et al., 2009) was referred to. The storage site area locality had some limited in situ stress data shown.
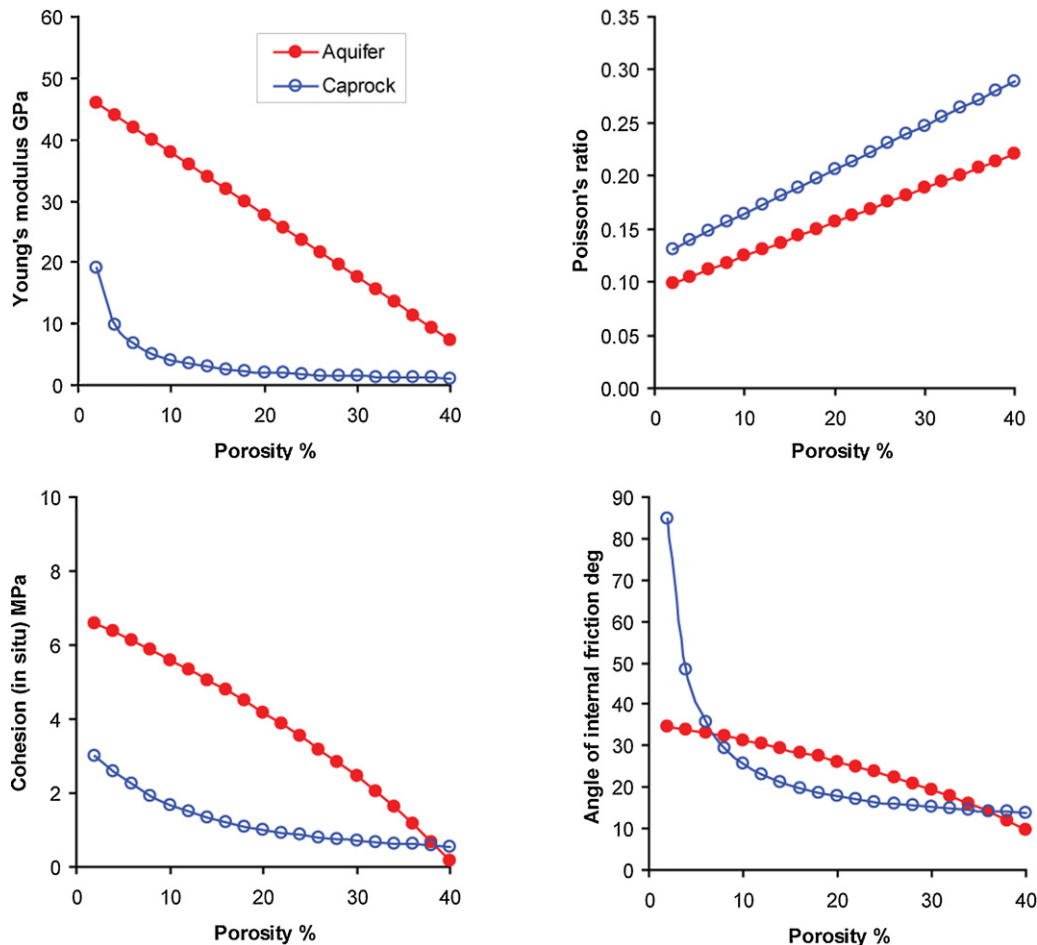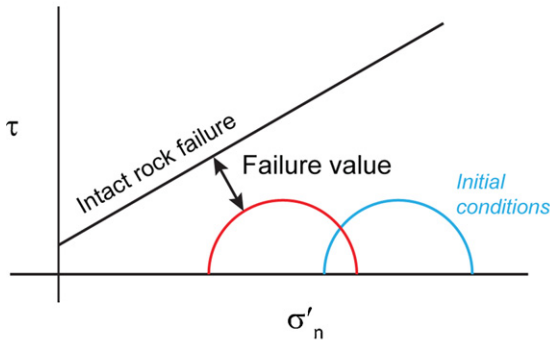

Fig. 4. Geomechanical properties correlations used in models based on published data.

(a) *This case is for illustrative purposes only – normally the Mohr circle would not move without changing size in a real injection scenario.*

(b) *This case is illustrative of injection in a strike slip stress regime where the Mohr circle enlarges due to the poroelastic effect.*
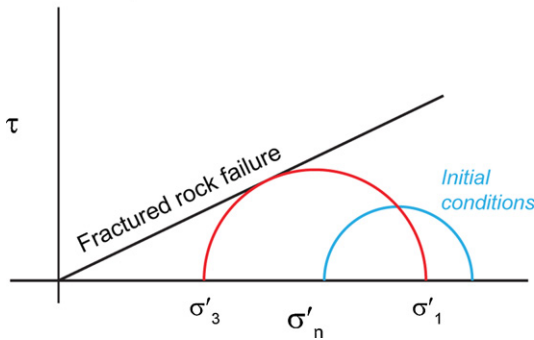
Fig. 5. Illustrations of Mohr–Coulomb shear failure: (a) the case of a pore pressure induced change with injection moving the stress state towards the intact rock failure envelope and (b) the case of a poroelastic change moving the stress state toward the fractured rock failure envelope (fault reactivation).

From the orientation of nearby unclassified stress regime data it appeared reasonable to assume the maximum horizontal stress azimuth was in a direction of N 35° W. On the basis of other slightly remoter data it was also assumed that the stress regime at the site was strike-slip with a maximum horizontal stress S_{Hmax} equal to $1.5\,S_V$ and a minimum horizontal stress S_{hmin} equal to S_V where S_V is the vertical stress.

2.3. Geomechanical failure assessment

Fracturing of the intact rock can be analysed directly by examining a property termed the "failure value", available in Modeler. This property is a measure of the proximity of the stress state at a particular location to the failure envelope. The failure value is a large negative number when the stress state is remote from the failure envelope and becomes less negative the closer the stress state is to the failure envelope. At failure the value is zero.

A simple criterion for fault (fracture) reactivation through shear slip can be derived from the Mohr–Coulomb criterion. For cohesionless faults with a coefficient of friction of 0.6 (field observation lower value) this can be expressed as:

$$\sigma'_1 = 3\sigma'_3$$

i.e. shear slip would be induced wherever or whenever the maximum principal effective stress σ'_1 exceeds three times the minimum principal effective stress σ'_3 on preferentially oriented faults. Modeler can be used to calculate the ratio $(\sigma'_1/3\sigma'_3)$ which will be unity at failure. These features are illustrated in Fig. 5.

The geomechanical time step dates of the coupled simulation were chosen manually to correspond with significant changes in the aquifer pressure history. The models were run without and with presence of regional aquifers. These former types of systems will experience higher pressure changes with CO_2 injection, as mentioned above.
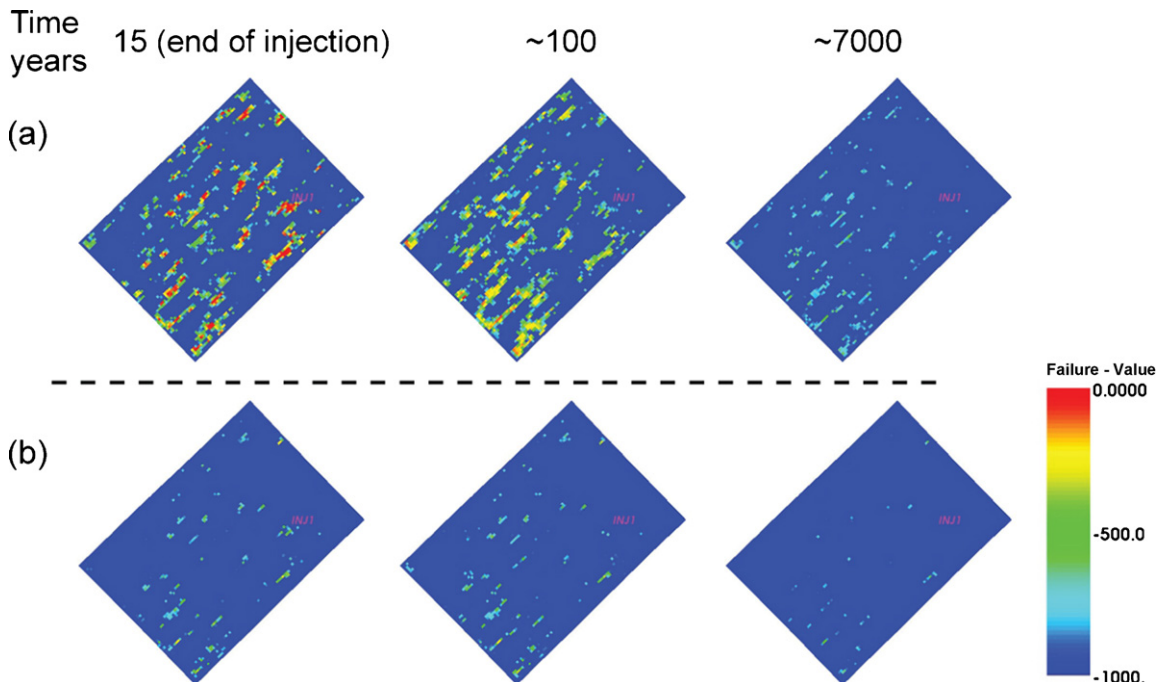

Fig. 6. Fine grid model – failure values predicted in caprock lower layer compared (a) without and (b) with regional aquifer connections.

3. Preliminary results

During the simulation without regional aquifer connections the average aquifer pressure increases up to the end of the injection period and then reduces as pressure equilibrates throughout the system. The initial average aquifer pressure was 10.4 MPa (ranging from 5.0 MPa to 15.3 MPa) and increased to 12.2 MPa after 15 years injection, reducing to initial 11.5 MPa after ~7000 years.

The modelling results are presented as time sequenced areal plots of failure and slip calculation values for the lower caprock and upper aquifer layers (other layers were examined but are not discussed here as the main effects were in these layers). Also for simplicity and to aid interpretation a reduced subset of the geomechanical timesteps has been plotted. The location of the injector in the plots is indicated by "INJ1".

Fig. 6(a) shows the initial failure value results for the fine grid model indicating the potential for incipient fracture (shear failure) as predicted by the Mohr–Coulomb failure criterion. The results can be interpreted as follows: blue – non-failed, red – at or near failure. Temporally, the maximum effect is in the lower caprock at the end of injection (15 years), with significant patches of cells indicating failure. The effects reduce but persist at later timesteps as the pressure response equilibrates throughout the aquifer/caprock system. Spatially the effects are slightly more pronounced in the up-dip region (south-west) but not markedly so because of very slight dip angle. The distributions are heterogeneous because of the stochastic variations in porosity in the geological model. Regions of high porosity are closer to failure.

It should also be noted that for the failure value results, the in situ cohesion values are dependent on the in situ strength factor used. Here an in situ strength factor of 5 has been assumed, when calculating in situ UCS values from laboratory UCS values which considerably reduces the material in situ cohesion.

The slip calculation results – potential for (strike-slip) fault reactivation in the upper aquifer layer – for the fine grid model are shown in Fig. 7(a). The results can be interpreted as follows: blue – non-slip, red – calculation value unity i.e. slipping on preferentially aligned faults. An initial perturbation occurs in the region of the injector (light blue area) in the early stage of injection but as the aquifer pressure increases and the principal effective stress magnitudes change this disappears and the main effect is seen in the up-dip part of the model (red area) with slip predicted.

Again, as the pressure response equilibrates throughout the aquifer/caprock system – the faults are not continuous barriers to flow – this effect also disappears. Spatially these effects are not so localised as the failure value results because they do not depend on the intact rock failure properties. In this case, although reactivation of faults is predicted by the model the region where this occurs is remote from the CO_2 plume and therefore does not pose a threat to storage integrity.

The effects of running the fine grid model with regional aquifer connected support are shown in Figs. 6(b) and 7(b). It can be seen that both the results for the models are spatially and temporally the same with the only difference being the magnitude of the results. For the model with regional aquifer connections there is no actual failure predicted (red colour) but cells approaching failure correspond exactly to those up-dip with high porosity as in the model without regional aquifer connections. Essentially the effect of the regional aquifer connections is to reduce the increases in pore pressure with injection and thereby ameliorate the geomechanical effects.

These results underline the importance of modelling regional aquifer support accurately in models of CO_2 geological storage since this significantly affects the pressure and hence geomechanical response.

4. Rock mechanics laboratory data

A suite of rock mechanics laboratory tests was carried out on 12 1½ inch diameter cylindrical rock samples produced from core recovered from a borehole in the target formations near the proposed storage site. The samples covered a porosity range 8.9–29.7%, and a permeability range 0.9–3546 mD for the aquifer (sandstone) material. Two samples only of the caprock (mudstone) material were tested with porosity 1.5 and 5.2%. Due to the vagaries of
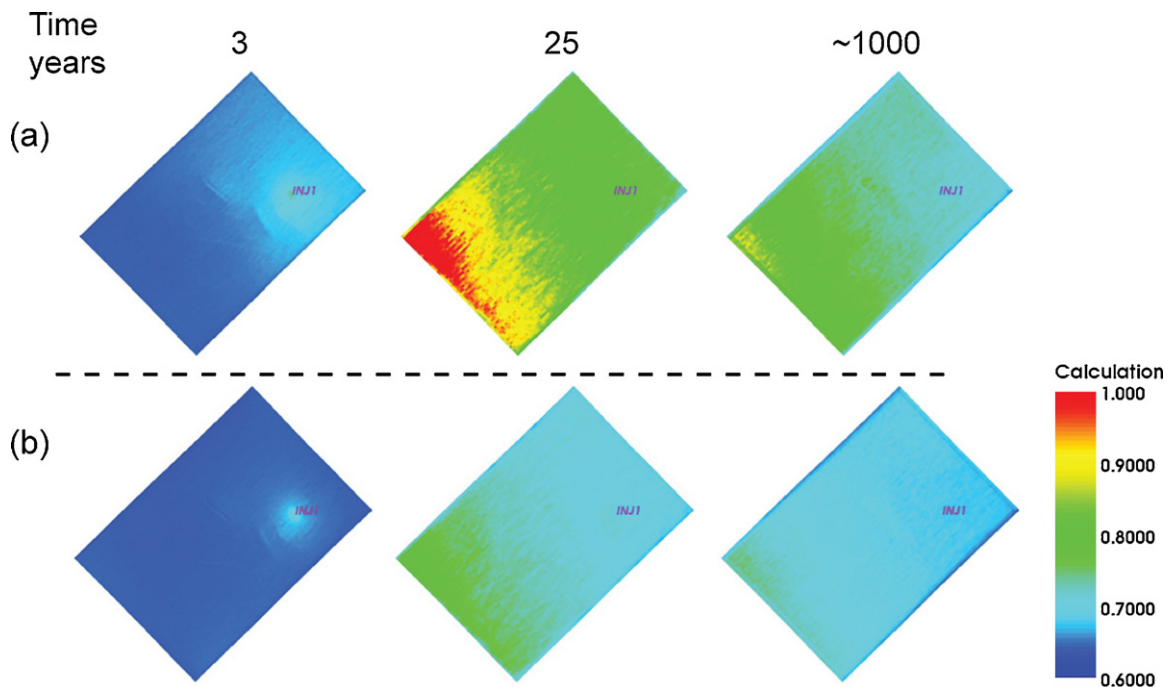

Fig. 7. Fine grid model–slip calculation values predicted in top aquifer layer compared (a) without and (b) with regional aquifer connections.

Table 2
Initial mean effective stress ranges and in situ permeability reduction factors.

Parameter	Minimum	Maximum	Average
Initial mean effective stress (MPa)			
Caprock	5.85	20.60	14.34
Aquifer	9.00	26.10	17.99
In situ permeability reduction factor			
Aquifer	0.596	0.719	0.629

Note: the minimum permeability reduction factor (greatest reduction) corresponds to maximum stress value and vice versa.

laboratory testing the complete suite of tests was not carried out on all the samples.

The samples were strain gauged enabling measurements of the static elastic constants to be made under triaxial stress conditions in a Hoek cell. Simultaneous measurements of the dynamic elastic constants were made using a piezoelectric ultrasonic pulse system. The tests were performed first on the dry samples and then subsequently the samples were fully saturated in brine and tested again. The second set of tests enabled changes in permeability with stress to be measured, however this time only the dynamic elastic constants could be measured. The saturated samples were then tested to (shear) failure using the multi-failure state method.

The laboratory measurements of geomechanical properties were analysed and compared to the properties used in the preliminary geomechanical models. The analysis of the measurements was carried out in three parts: deformation properties (Young's modulus and Poisson's ratio), failure properties (in situ cohesion and angle of internal friction) and permeability sensitivity to stress (aquifer rock only).

4.1. Rock deformation properties

The rock deformation data consisted of static and dynamic measurements on dry and 100% brine saturated rock samples. The analysis procedure was as follows:

1. A power law was fitted to the measurements for each sample/property combination, as shown in the examples given in Fig. 8.
2. An average mean effective stress, determined by the geomechanical stress initialisation for the updated models was used to determine the geomechanical property for that particular sample – classified as either aquifer or caprock – at in situ conditions from the curve fit equation. The average mean effective stress values are given in Table 2. This gave a set of datum points for the sample also shown in Fig. 8.
3. Using the ambient porosity of the sample, the geomechanical property datum values could then be compared to the correlations used in the preliminary models as shown in Fig. 9.

The aquifer samples covered a good range of porosity and the fitted curves showed typical differences to be expected depending on the property/condition of the rock i.e. dynamic Young's modulus values are higher than static values and also increased again with fluid saturation. The values actually required for the models – static, brine saturated condition – were not explicitly available from the laboratory data, but the preliminary Young's modulus correlations looked satisfactory, whereas the Poisson's ratio correlations looked as if they may have been under-estimated. This data is shown in Fig. 9(a).

There were limited measurements for the few caprock (mudstone) samples – the porosities being at the low end of the scale, covering a very narrow porosity range. However, the Young's modulus preliminary correlations again appeared satisfactory,
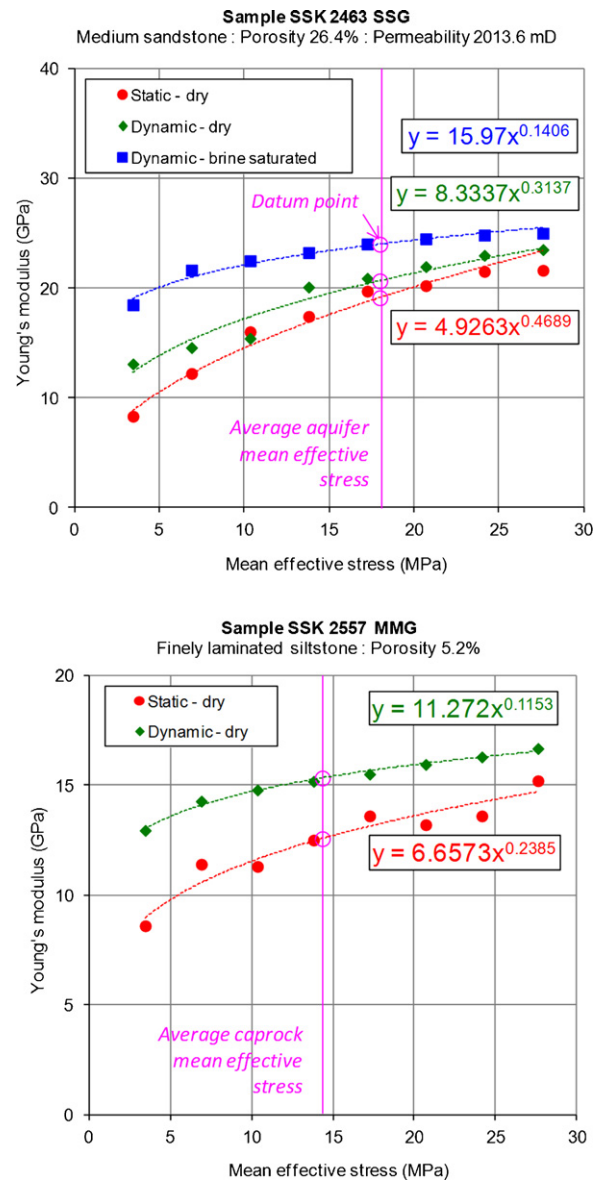

Fig. 8. Examples of laboratory measurements of geomechanical properties with curve fits used to determine datum points at average aquifer and caprock mean effective stress conditions.

whilst the Poisson's ratio correlations may also have been under-estimated. This data is shown in Fig. 9(b).

4.2. Rock failure properties

The rock failure properties were taken from multi-failure state testing data on brine saturated samples. The calculated Mohr-Coulomb cohesion values were again adjusted to in situ cohesion values using an in situ strength factor of 5. The values of in situ cohesion and angle of internal friction could then be compared to the correlations used in preliminary models as shown in Fig. 9(c).

Again, there are few data points, particularly for the caprock material, however there seems to be reasonable agreement with the preliminary correlations for in situ cohesion of the caprock material and angle of internal friction of the aquifer material. The derived in situ cohesion values of the aquifer material from the laboratory measurements indicate that the preliminary correlations have under-estimated this whereas the angle of internal
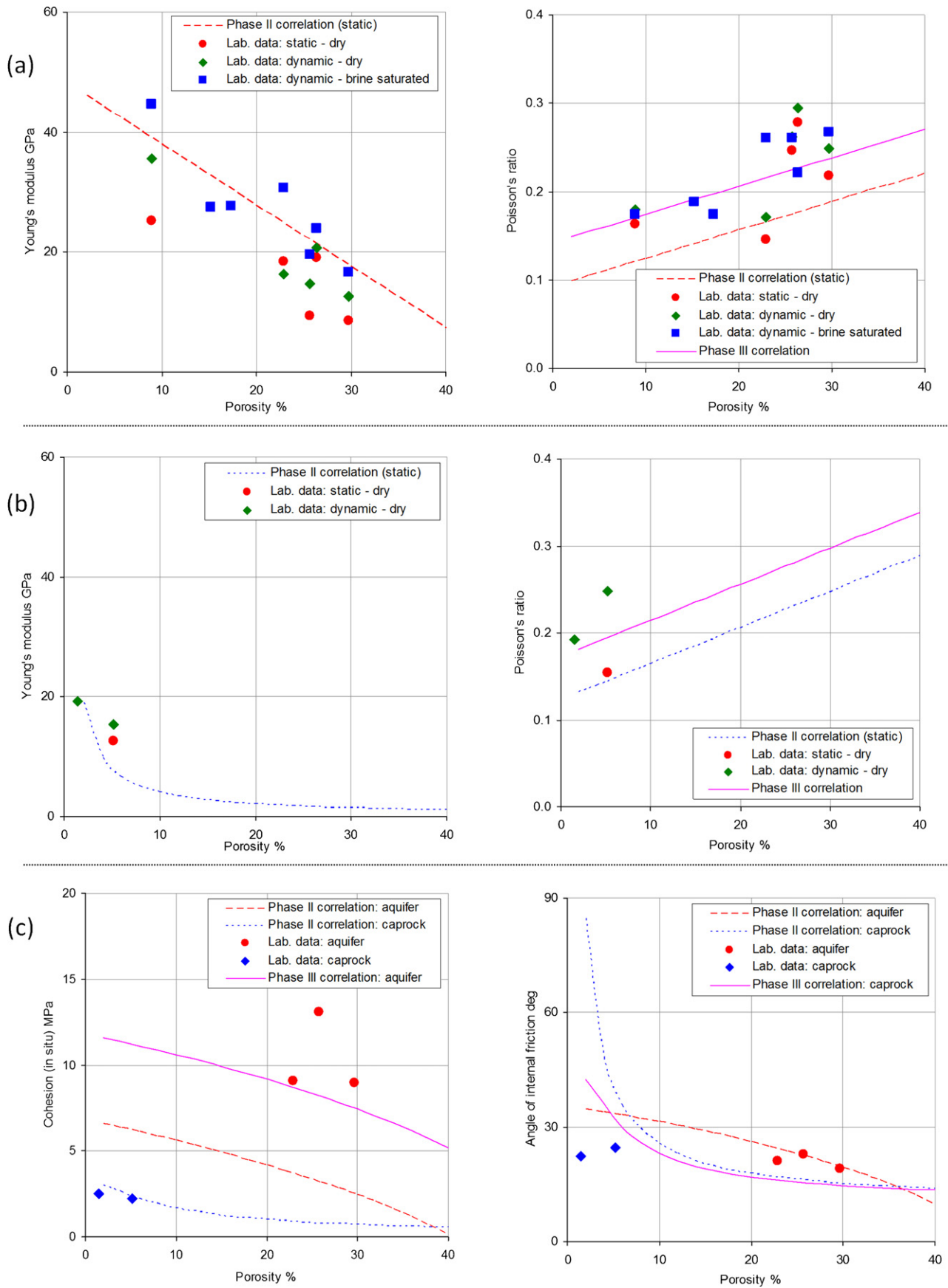
Fig. 9. Comparisons of geomechanical properties measured in the laboratory with porosity correlations used in the preliminary models – (a) aquifer deformation, (b) caprock deformation and (c) aquifer and caprock failure. The modified correlations [continuous (purple) lines] used in the updated models are also shown. (For interpretation of the references to colour in this figure legend, the reader is referred to the web version of the article.)

Table 3
Summary of modifications made to geomechanical property correlations.

Property	Aquifer	Caprock
Young's modulus	No change	No change
Poisson's ratio	Shift correlation to increase all values by 0.05	Shift correlation to increase all values by 0.05
Cohesion (in situ)	Shift correlation to increase all values by 5 MPa	No change
Angle of internal friction	No change	Shift correlation to decrease values systematically with greater reduction at lower porosity

Fig. 10. Laboratory measurements of permeability stress sensitivity, fitted average curves and aquifer mean effective stress ranges.

friction of the caprock material has been over-estimated. Modifying the former parameter i.e. increasing the in situ cohesion will have ameliorating effects on failure of intact rock in the aquifer, but reducing the latter parameter is likely to have detrimental effects i.e. increasing likelihood of failure of intact rock in the caprock.

4.3. Correlation modifications

The geomechanical property correlations for the updated models were modified from those used in the preliminary models. These modifications are summarised in Table 3 and also shown on the plots presented in Fig. 9.

For the deformation properties only changes were made to the Poisson's ratio correlations of both the aquifer and caprock – these would be expected to have a small effect on the models.

For the failure properties, the in situ cohesion values of the aquifer material was increased (this would reduce the potential for failure) whilst the angle of internal friction of the caprock material was decreased (increasing the potential for failure). The latter correlation was tentatively modified (on the basis of very limited laboratory data), as very small changes to the angle of internal friction can make large differences in the potential for geomechanical (shear) failure.
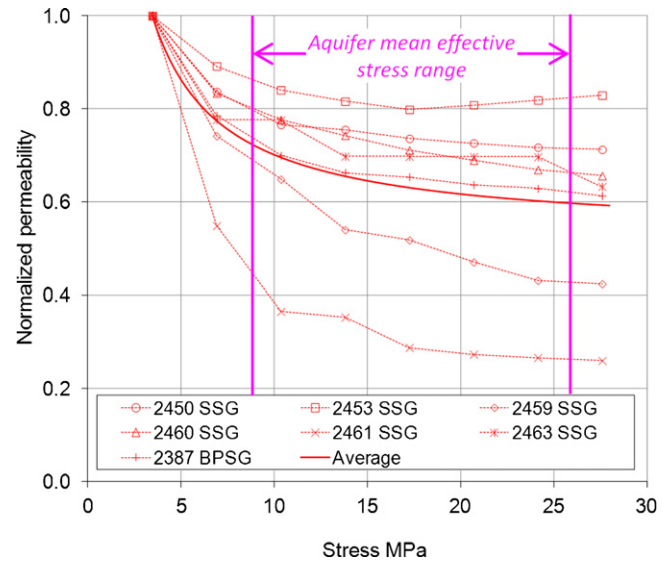
4.4. Permeability stress sensitivity

The permeability stress sensitivity data was taken from triaxial tests on 100% formation brine saturated sandstone samples. The available data is shown plotted in Fig. 10. A power law curve was fitted to the averaged data. This curve was used to calculate permeability reduction factors depending on mean effective stress, deriving initial in situ permeabilities for the updated geomechanical models. The initial mean effective stresses were exported from the geomechanical models, used to calculate modified permeabilities and then these re-imported as in situ permeabilities on a cell by cell basis for the models. The overall ranges of permeability reduction factors for the models are given in Table 2.
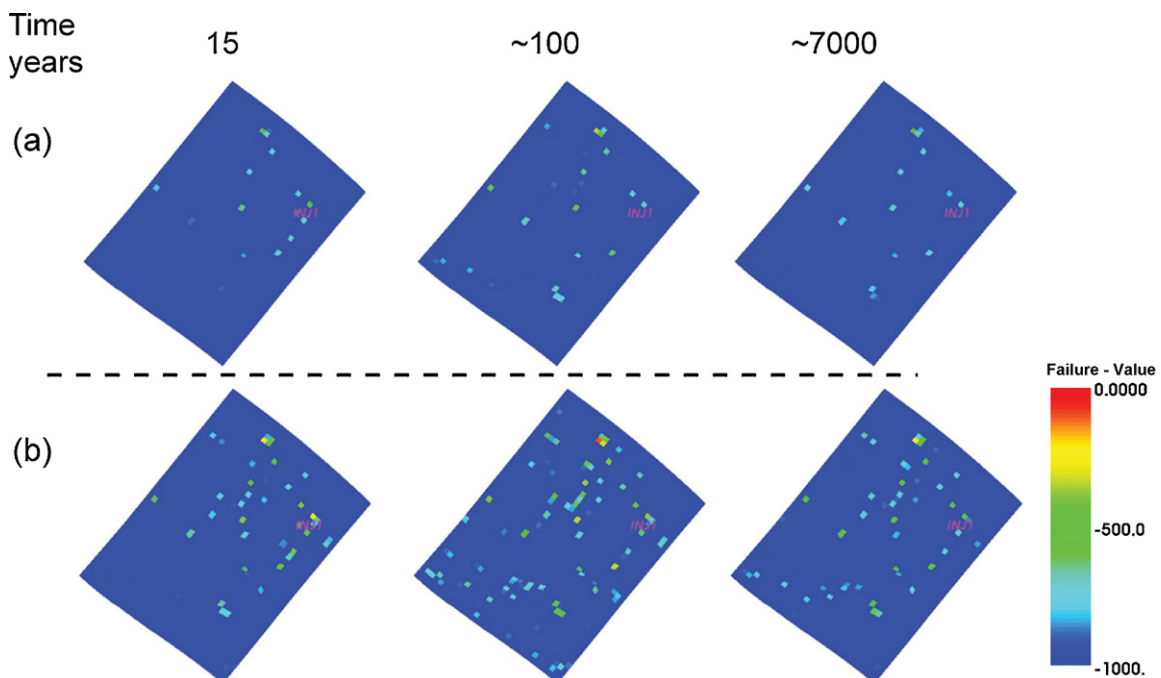

Fig. 11. Coarse grid model – failure values predicted in the lower caprock layers compared (a) with preliminary property correlations and (b) with modified correlations.

5. Re-development of models and updated results

The geomechanical models were re-developed from the reservoir simulation models developed for final phase of the CASSEM project. These reservoir simulation models incorporated changes made to the porosity and permeability realisations although the geometry remained the same. The previous workflow was changed slightly to include the requirement to incorporate initial in situ permeabilities. Both fine and coarse grid models were developed with the same grid statistics as previously. The fine grid model was only run in stress initialisation mode to calculate the mean stress values required to derive the permeability reduction factors for use in the flow simulation studies.

The modified geomechanical properties for the models were assigned to the various regions (side/under/overburden, aquifer, caprock) of the models as previously, there being no changes to the number and differentiation of the layers of the reservoir models. The stress initialisation parameters of the models were also the same as previously. The input permeabilities were modified from ambient to in situ stress conditions using the laboratory derived average permeability stress sensitivity curves. Exactly the same timesteps were used in the geomechanical simulations as for the preliminary models. The up-dated geomechanical models were then run with the both the preliminary and up-dated geomechanical property correlations.

The pressure response of the system during the simulation was very similar to the preliminary model. The initial average aquifer pressure was 10.4 MPa, increasing to 12.2 MPa at the end of injection and reducing to 11.7 MPa after ∼7000 years.

The intact rock failure results shown in Fig. 11 are very similar to those obtained in the preliminary modelling. The differences are due to different realisations of the porosity and permeability distributions. These changes have slightly altered the pressure response which has affected the failure response of the system.

It can be seen that there is still a temporal aspect, with failure apparent initially in the caprock lower layer persisting after injection ceases and pressure equilibrates throughout the system. The modifications to the geomechanical property correlations make the caprock marginally more susceptible to failure. No intact failure was detected in the aquifer.

The slip calculation (fault reactivation) results shown in Fig. 12 are very similar and also virtually identical to the preliminary results. This is not surprising since the fault reactivation calculation depends on the effective stress state and is independent of the intact failure properties. These and the intact rock failure results indicate the relative benignness of this site for CO_2 geological storage as regards geomechanical integrity.

6. Conclusions

Proof of geomechanical structural integrity of storage sites will be an important factor in the successful deployment of CCS. Given the uniqueness of potential storage sites this will need to be assessed on a case by case basis. Coupled reservoir simulation and geomechanical modelling will be one of the techniques used to achieve this. Simulation methods currently used in hydrocarbon extraction provide suitable tools but these will need to be adapted for CO_2 geological storage work together with site specific rock sample data, including the measurement of site specific geomechanical properties.

The work reported here endeavours to explore this process. The geomechanical modelling was carried out using different models with two grid resolutions. Correlations between rock deformation and failure parameters and porosity were developed and used to populate the geomechanical models. Assumptions were made about the in situ stress state and modelling results were used to make predictions about the likely timing and extent of both failure of the intact rock and reactivation of faults within the layers comprising the aquifer and caprock of a potential storage site.

Predictions of failure of the intact rock and reactivation of faults in the models show different characteristics. Failure of the intact rock is closely associated with regions of weak rock (high porosity) within the models together with the lesser influence of depth (which determines the relative magnitudes of the in situ stresses). These characteristics are in turn influenced by the porosity realisations generated in the underlying geological model and the in situ
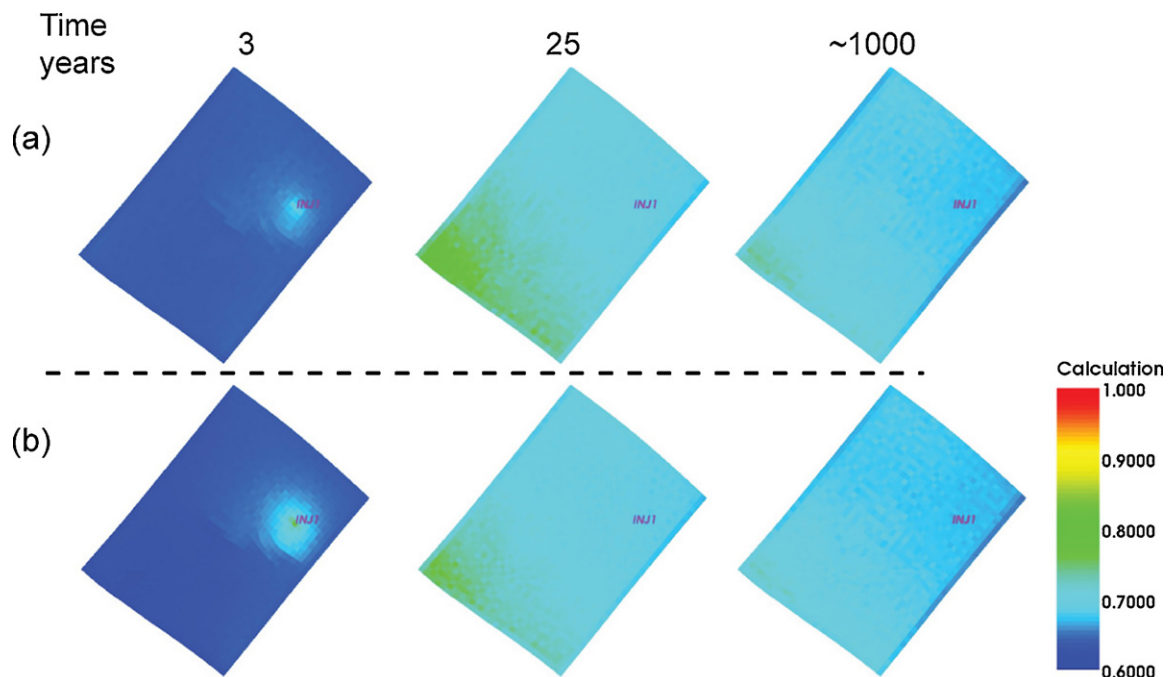

Fig. 12. Coarse grid model – slip calculation values predicted in aquifer top layers compared (a) with preliminary property correlations and (b) with modified correlations.

strength factor used to scale up laboratory UCS to reservoir (in situ) UCS. Reactivation of faults is independent of the failure (porosity) characteristics of the models and is primarily determined by the relative magnitudes of the minimum and maximum effective stresses. For the site modelled here fault reactivation was only predicted in the case of a contained system with unrealistically high pressure increase and at a location remote from the CO_2 plume. In this strike-slip stress regime, optimally orientated faults for reactivation would be reverse faults.

The laboratory rock mechanics data was analysed and the derived geomechanical properties integrated in to the site geomechanical models, effectively tuning the porosity correlations used in the preliminary models.

The initial modelling showed the subtleties in intensity of potential, location and timing of possible failure of both the caprock and aquifer rock for the proposed storage sites. However the changes in the updated results illustrate the most important conclusion that can be drawn from the geomechanical modelling is the significance of realistic and accurate pressure response prediction on the induced geomechanical response of the storage system.

The presence of regional aquifer connections has a direct effect on the pressure response and hence geomechanical response of the storage system. Geomechanical effects are ameliorated in systems which are connected to regional aquifer i.e. not contained.

It is also recognised that a limited geomechanical analysis was carried out which did not consider the effects of faults and fractures modelled more directly, to achieve a feedback in the flow response to strain induced permeability changes on faults.

Acknowledgements

References

Bissell, R.C., Vasco, D.W., Atbi, M., Hamdani, M., Okwelegbe, M., Goldwater, M.H., 2011. A full field simulation of the in Salah gas production and CO_2 storage project using a coupled geo-mechanical and thermal fluid flow simulator. Energy Procedia 4, 3290–3297.

Cappa, F., Rutqvist, J., 2011. Modeling of coupled deformation and permeability evolution during fault reactivation induced by deep underground injection of CO_2. International Journal of Greenhouse Gas Control 5, 336–346.

Edlmann, K., 2001. A new methodology for predicting the geomechanical properties of clastic reservoir rocks, Ph.D. Thesis, Heriot-Watt University, Edinburgh.

Heidbach, O., Tingay, M., Barth, A., Reinecker, J., Kurfeß, D., Müller, B., 2009. The World Stress Map Database Release 2008. Helmholtz Centre Potsdam – GFZ German Research Centre for Geosciences.

Horsrud, P., 2001. Estimating mechanical properties of shale from empirical correlations. SPE Drilling & Completion, 68–73.

Horsrud, P., Sønstebø, E.F., Bøe, R., 1998. Mechanical and petrophysical properties of North Sea Shales. International Journal of Rock Mechanics and Mining Science 35, 1009–1020.

Jimenez, J.A., Chalaturnyk, R.J., Whittaker, S.G., 2005. A mechanical earth model for the Weyburn CO_2 monitoring and storage project and its relevance to long-term performance assessment. In: Rubin, E.S., Keith, D.W., Gilboy, C.F., Wilson, M., Morris, T., Gale, J., Thambimuthu, K. (Eds.), Greenhouse Gas Control Technologies, vol. 7. Elsevier Science Ltd, Oxford, pp. 2141–2145, 5–9 September 2004, Vancouver, Canada.

Lucier, A., Zoback, M., Gupta, N., Ramakrishnan, T.S., 2006. Geomechanical aspects of CO_2 sequestration in a deep saline reservoir in the Ohio River Valley region. Environmental Geosciences 13, 85–103.

Morris, J.P., Hao, Y., Foxall, W., McNab, W., 2011. A study of injection-induced mechanical deformation at the In Salah CO_2 storage project. International Journal of Greenhouse Gas Control 5, 270–280.

Morris, J.P., McNab, W.W., Johnson, S.M., Hao, Y., 2009. Coupled hydromechanical and reactive transport processes with application to carbon sequestration. In: 43rd U.S. Rock Mechanics Symposium & 4th U.S. – Canada Rock Mechanics Symposium, June 28–July 1. American Rock Mechanics Association, Asheville, North Carolina.

Pickup, G.E., Jin, M., Olden, P., Mackay, E.J., Sohrabi, M., 2011. A sensitivity study on CO_2 storage in saline aquifers. In: SPE EUROPEC/EAGE Annual Conference and Exhibition, Vienna, Austria.

Preisig, M., Prévost, J.H., 2011. Coupled multi-phase thermo-poromechanical effects. Case study: CO_2 injection at In Salah, Algeria. International Journal of Greenhouse Gas Control 5, 1055–1064.

Ringrose, P., Atbi, M., Mason, D., Espinassous, M., Myhrer, Ø., Iding, M., Mathieson, A., Wright, I., 2009. Plume development around well KB-502 at the In Salah CO_2 storage site. First Break 27, 85–89.

Rutqvist, J., 2012. The geomechanics of CO_2 storage in deep sedimentary formations. Geotechnical & Geological Engineering 30, 525–551.

Rutqvist, J., Birkholzer, J., Cappa, F., Tsang, C.F., 2007. Estimating maximum sustainable injection pressure during geological sequestration of CO_2 using coupled fluid flow and geomechanical fault-slip analysis. Energy Conversion and Management 48, 1798–1807.

Rutqvist, J., Birkholzer, J.T., Tsang, C.-F., 2008. Coupled reservoir-geomechanical analysis of the potential for tensile and shear failure associated with CO_2 injection in multilayered reservoir-caprock systems. International Journal of Rock Mechanics and Mining Sciences 45, 132–143.

Rutqvist, J., Tsang, C.F., 2002. A study of caprock hydromechanical changes associated with CO_2 injection into a brine formation. Environmental Geology 42, 296–305.

Rutqvist, J., Vasco, D.W., Myer, L., 2009. Coupled reservoir-geomechanical analysis of CO_2 injection at In Salah, Algeria. Energy Procedia 1, 1847–1854.

Rutqvist, J., Vasco, D.W., Myer, L., 2010. Coupled reservoir-geomechanical analysis of CO_2 injection and ground deformations at In Salah, Algeria. International Journal of Greenhouse Gas Control 4, 225–230.

Schlumberger, 2009. The VISAGE System: User's Guide.

Smith, M., Campbell, D., Mackay, E., Polson, D. (Eds.), 2011. CO_2 Aquifer Storage Site Evaluation and Monitoring – Understanding the challenges of CO_2 storage: results of the CASSEM project. Scottish Carbon Capture and Storage, ISBN 978-0-9571031-0-8 http://www.sccs.org.uk/working-papers.html#cassem

Streit, J.E., Hillis, R.R., 2002. Estimating fluid pressures that can induce reservoir failure during hydrocarbon depletion. In: SPE/ISRM Rock Mechanics Conference, Irving, TX, 20–23 October 2002.

Streit, J.E., Hillis, R.R., 2003. Building geomechanical models for the safe underground storage of carbon dioxide in porous rock. In: Gale, J., Kaya, Y. (Eds.), Greenhouse Gas Control Technologies – 6th International Conference. Pergamon, Oxford, Kyoto, Japan, 1–4 October 2002, pp. 495–500.

Streit, J.E., Hillis, R.R., 2004. Estimating fault stability and sustainable fluid pressures for underground storage of CO_2 in porous rock. Energy 29, 1445–1456.

Streit, J.E., Siggins, A.F., 2005. Predicting and monitoring and controlling geomechanical effects of CO_2 injection. In: 7th International Conference on Greenhouse Gas Control Technologies (GHGT-7). Elsevier Science Ltd, Vancouver, Canada, 5–9 September 2004, p. 643.

Streit, J.E., Siggins, A.F., Evans, B.J., 2005. Chapter 6 – Predicting and monitoring geomechanical effects of CO_2 injection. In: Benson, S.M. (Ed.), Carbon Dioxide Capture for Storage in Deep Geologic Formations – Results from the CO_2 Capture Project. Elsevier Science, Amsterdam, pp. 751–766.

Wilson, A.H., 1982. Soft Rock Mechanics. NCB Mining Research and Development Establishment.

Zoback, M.D., Barton, C.A., Brudy, M., Castillo, D.A., Finkbeiner, T., Grollimund, B.R., Moos, D.B., Peska, P., Ward, C.D., Wiprut, D.J., 2003. Determination of stress orientation and magnitude in deep wells. International Journal of Rock Mechanics and Mining Sciences 40, 1049–1076.